Journal of Materials Chemistry A

Accepted Manuscript

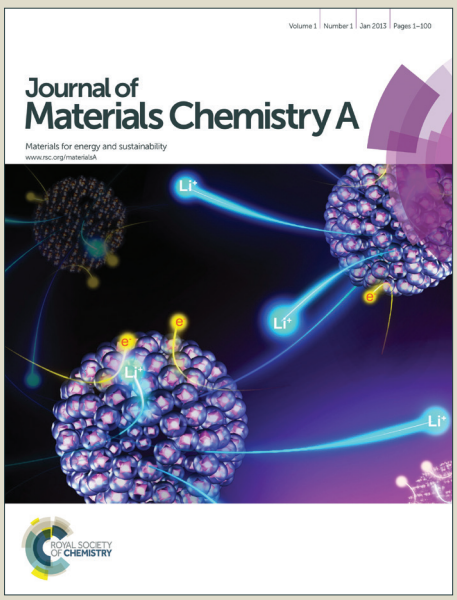

ROYAL SOCIETY OF CHEMISTRY

www.rsc.org/materialsA

Journal of Materials Chemistry A RSCPublishing

PAPER

Iron-containing, High Aspect Ratio Clay as Nanoarmor that Imparts Substantial Thermal/Flame Protection to Polyurethane with a Single Electrostatically-deposited Bilayer

A.A. Cain,[a] M.G.B. Plummer,[a] S.E. Murray,[a] L. Bolling,[a] O. Regev,[b] and J.C. Grunlan[a]

Cite this: DOI: 10.1039/x0xx00000x

Received 10th July 2014,

DOI: 10.1039/x0xx00000x

www.rsc.org/

In an effort to impart fire protection properties to polyurethane foam using environmentally-benign components, layer-by-layer assembly is used to fabricate nanobrick wall thin films of branched polyethylenimine (PEI), chitosan (CH), and sodium montmorillonite (MMT) (or formulated vermiculite (VMT)) clay bricks. Using specially formulated, large-aspect-ratio VMT platelets, a single polymer/clay bilayer deposited on polyurethane foam (3.2 wt.% addition) was able to cut the peak heat release rate in half, reduce smoke release, and eliminate melt dripping. It takes 4 polymer/MMT bilayers to match these flame retardant properties and weight gain, indicating that nanoplatelet aspect ratio significantly enhances the nanocoating's ability to reduce heat transfer and prevent mass loss. This study demonstrates a simple, commercially viable, and effective fire protection alternative. Desirable fire performance properties for polyurethane foam no longer have to come at the cost of laborious, multi-step coating procedures or in choosing halogenated additives that are currently being scrutinized due to their potentially adverse effects to human health.

Introduction

Layer-by-layer (LbL) assembly has become a popular technique to fabricate polyelectrolyte-based thin films due to the nanoscale control of composition, tunable properties, and ease of fabrication from water.[1-4] The term 'nanobrick wall' was coined for LbL-deposited polymer/clay nanocomposites because the microstructure is created through alternate adsorption of cationic polymeric mortar and highly oriented anionic clay platelets (i.e., nanobricks).[5-10] When deposited on a polyester substrate, a 51 nm thick film generated the lowest oxygen permeability ever reported for a polymer/clay composite ($\leq 5x10^{-22}$ $cm^3(STP)•cm$ ($cm^{-2}•s^{-1}•Pa^{-1}$)).[11] This barrier surpasses completely inorganic SiOx (a commonly used barrier layer for plastic packaging films) by two orders of magnitude. As modeled by Cussler,[12] this layered polymer/clay structure creates a tortuous path through which gas molecules must travel. The diffusion path can be altered through precise tailoring of the thin film architecture (i.e., polymer mortar composition/thickness and clay spacing/packing/aspect ratio).[10,13,14] Aside from their obvious promise for packaging applications, these polymer/silicate LbL multilayers are also being investigated for their mechanical properties[15-18] and a variety of end-use applications such as diffusion barriers,[19,20] sensors,[21,22] drug delivery,[23-25] and fire protection.[26-29]

Rigid polyurethane (PU), which is widely used in the building industry due to its heat insulating properties, and flexible polyurethane, commonly used in upholstered furniture, are highly flammable materials susceptible to fast flame-spread and high heat release. Additionally, polyether and polyester units thermally degrade and regenerate isocyanate and diol precursor groups, producing harmful smoke and combustion products.[30] Inspiration for applying these nanobrick wall coatings to polyurethane foam as flame retardant (FR) came from the final stage of a schematic representation of a mechanism for flame suppression in melt-mixed ethylene-vinyl acetate and montmorillonite (MMT) clay,[31] which depicts a physical barrier created from the build-up of impermeable flakes and carbonized char. It was believed that ordered clay-polymer layers, deposited only on the surface, would more immediately act as a heat shield and interfere with the combustion cycle. This would eliminate engineering concerns associated with silicate dispersion within the material that adversely affect mechanical behavior. Nanobrick wall coatings have recently been developed to thwart the two key problems of polyurethane foam exposed to a heating source:[32-35] melt dripping and heat release.[36] In one case, a nine-layer system (three trilayers of poly(acrylic acid) (PAA)/polyethylenimine (PEI)/MMT) that resulted in a 4.8 wt.% nanocoating on foam, reduced peak heat release rate (pkHRR) by 70%.[37] This system is a condensed phase flame retardant, which

means the pyrolysis process and mass loss rate are slowed through the formation of carbonaceous-silicate char. Despite their promise, the numerous layers required to impart sufficient flame retardant behavior is daunting for practical use.

In an effort to create a flame retardant nanocoating for polyurethane foam with relatively few layers, montmorillonite clay and vermiculite clay were chosen as building blocks for nanobrick wall assemblies. The influence of clay aspect ratio and composition on fire behavior was studied as a function of layers deposited and nanocoating weight addition. It was found that a single PEI/VMT bilayer (BL) can achieve a 54% reduction in pkHRR and a 31% reduction in total smoke release (TSR), in comparison to uncoated polyurethane foam. Adding a second bilayer further reduces pkHRR and cuts the amount of smoke released by another 40%. Four nanobrick wall bilayers made with standard MMT clay are needed to match the weight gain and performance of a single vermiculite-based bilayer, which is attributed to complex interfacial interactions that occur between the components during thin film construction and to insulating properties of the formulated VMT platelets during combustion. Although vermiculite has been previously used in bulk polymer matrices, or layered into nanobrick walls to reduce gas permeation,[38-42] this is the first report of VMT being used in LbL multilayer thin films for anti-flammable purposes. This ability to cut peak heat release rate in half with a single bilayer (just 3.2 wt.% added to the foam), using environmentally-benign ingredients, is a tremendous breakthrough. It is likely that this nanocoating technology could be used to protect many household items (e.g., upholstered furniture) in a safe, cost-effective manner.

Results and discussion

Layer-by-layer film growth on 2D and 3D surfaces

Chitosan (CH)/clay bilayers were initially deposited on silicon wafers, using branched polyethylenimine as the initial layer to improve adhesion, to measure thickness as a function of bilayers, as shown in Fig. 1. Films grew linearly as a function of the number of layers deposited for both clay systems, with VMT having a greater growth rate (~6.2 nm/2 BL) than MMT (~ 2.8 nm/2 BL). Not only do these thicknesses suggest deposited clay nanoplatelets are oriented parallel to the substrate, the data implies that clays adsorbed to the surface are well exfoliated (platelets are ~1 nm thick), which has previously been observed.[43] The same linear growth was observed when a quartz crystal microbalance was used to measure growth as a function of weight deposited, with VMT-based recipes generating heavier layers. VMT-based films also have higher clay loading (87 wt.%), which results in a more dense thin film (MMT-based thin films are composed of 78 wt.% clay).

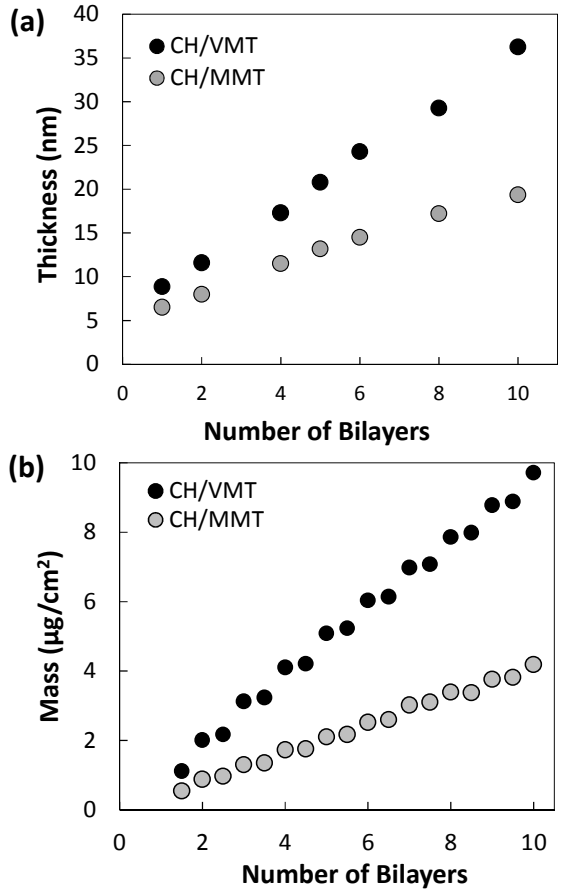

Fig. 1 a) Film thickness and b) mass as a function of bilayers deposited for polymer/clay assemblies. Ellipsometry was used to measure thickness, while QCM measured mass.

Coating three-dimensional, porous polyurethane required submersion into a PAA solution, whose pH was adjusted to 2 with nitric acid. This deposition step functions as a primer treatment that promotes nanocoating adhesion to the otherwise hydrophobic foam. The carboxylic acid pendant groups present on PAA have the ability to hydrogen bond through partial charge attraction with other polar groups on polyurethane. One and two bilayers of both clay-based recipes were then deposited on the foam, with PEI substituting for CH in the first cationic polyelectrolyte deposition. The MMT-based system was also evaluated at 4 BL to match the weight gain of 1 BL of the VMT-based system. Fig. 2 shows scanning electron microscope (SEM) images of the surface of uncoated foam, foam coated with a single layer of PEI, a single PEI/VMT BL, a single PEI/MMT BL, and 4 MMT-based BL. Uncoated polyurethane has a smooth surface (Fig. 2a), while several cracks can be seen in the PAA/PEI-primed foam (Fig. 2b) due to the glassy nature of this polyelectrolyte film.[13] The single polymer/clay bilayer coatings reveal excellent clay coverage over the polyurethane surface. Aspect ratios of the observed clusters are much larger than the reported aspect ratios for both VMT (1100) and MMT (200),[43,44] providing good evidence of aggregated clay platelets adhering well to the porous foam surface. Individual MMT platelets are not distinguishable in the 4 BL MMT-based coating systems (Fig. 2e).

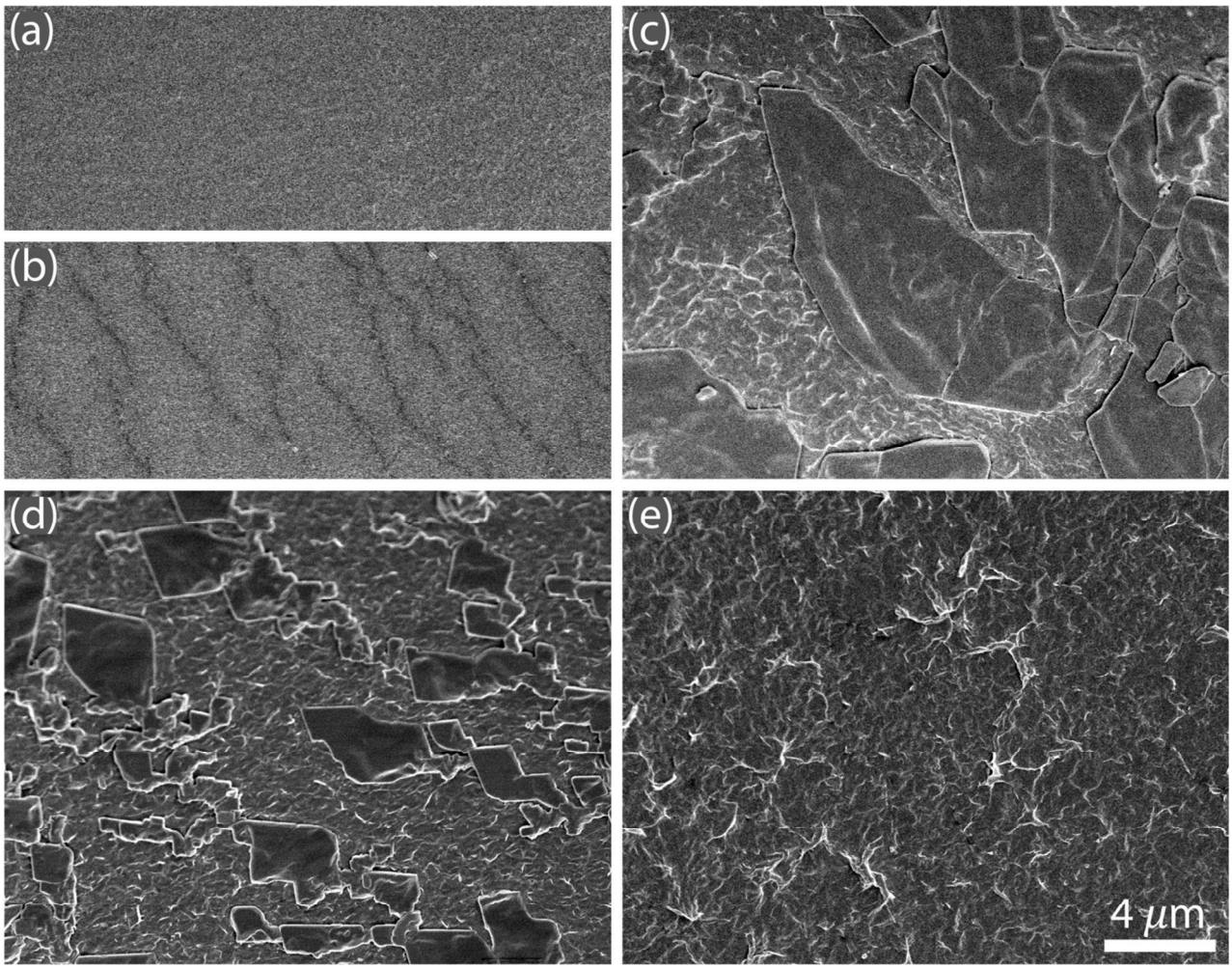

Fig. 2 SEM images of a) control foam, foam coated with b) a single layer of PEI, c) a single PEI/VMT bilayer, d) a single PEI/MMT bilayer, and e) a 4 BL MMT-based coating.

Fig. 3a and b shows SEM images of freeze-fractured samples at low and high magnification, which shows that the complex, irregular polyurethane matrix is fully coated with the VMT-based recipe at 1 BL and confirms the presence of clay aggregates within the coating. Fig. 3c shows high magnification transmission electron microscope (TEM) cross-sectional micrographs of these same single bilayer coatings deposited on the flexible foam. The source of contrast in these TEM micrographs is electron density, where materials with higher electron density (clay) appear darker than lower density materials (polymer). The image of the ordered layers also highlights that the largest dimension of the clay deposits parallel to the surface. As shown in Fig. 3c, several vermiculite platelets are deposited after a single deposition in the aqueous clay suspension, suggesting VMT clay is only partially exfoliated in solution and that stacks of clay deposit in the thin film. The same trend holds for the MMT-based recipe in Fig. 3d, e, and f. Fig. 3 also shows that the nanocoatings deposit much thicker on polyurethane than what was measured on flat silicon wafers. The observed differences are attributed to several factors: the influence of the PAA deposition on the deposited multilayers, the effects of the different coating procedures for 2D and 3D substrates, and the chemical nature of the substrates themselves.

Thickness of a deposited multilayer containing weak polyelectrolytes is strongly dependent upon the degree of ionization and conformation of both absorbed polymer and that of the previous layer.[45] When PAA-coated PU surfaces are immersed into PEI solutions at pH 10, there is an increase in surface charge density. It is well documented that PEI chains diffuse into deposited PAA layers when both polymers have a low degree of ionization.[46] The poly(acrylic acid) surface treatment step added to the foam coating procedure not only enhances adhesion between the polyurethane and subsequent layers, it promotes thick polyethylenimine deposition. The observed surface roughness is attributed to the rigorous coating process (involving full compression of the foam and multiple wringing steps). The complex porous structure of the polyurethane hinders thorough rinsing, where weakly bound polyelectrolytes and clay become trapped within the matrix, contributing to thicker deposition and rougher deposited layers.

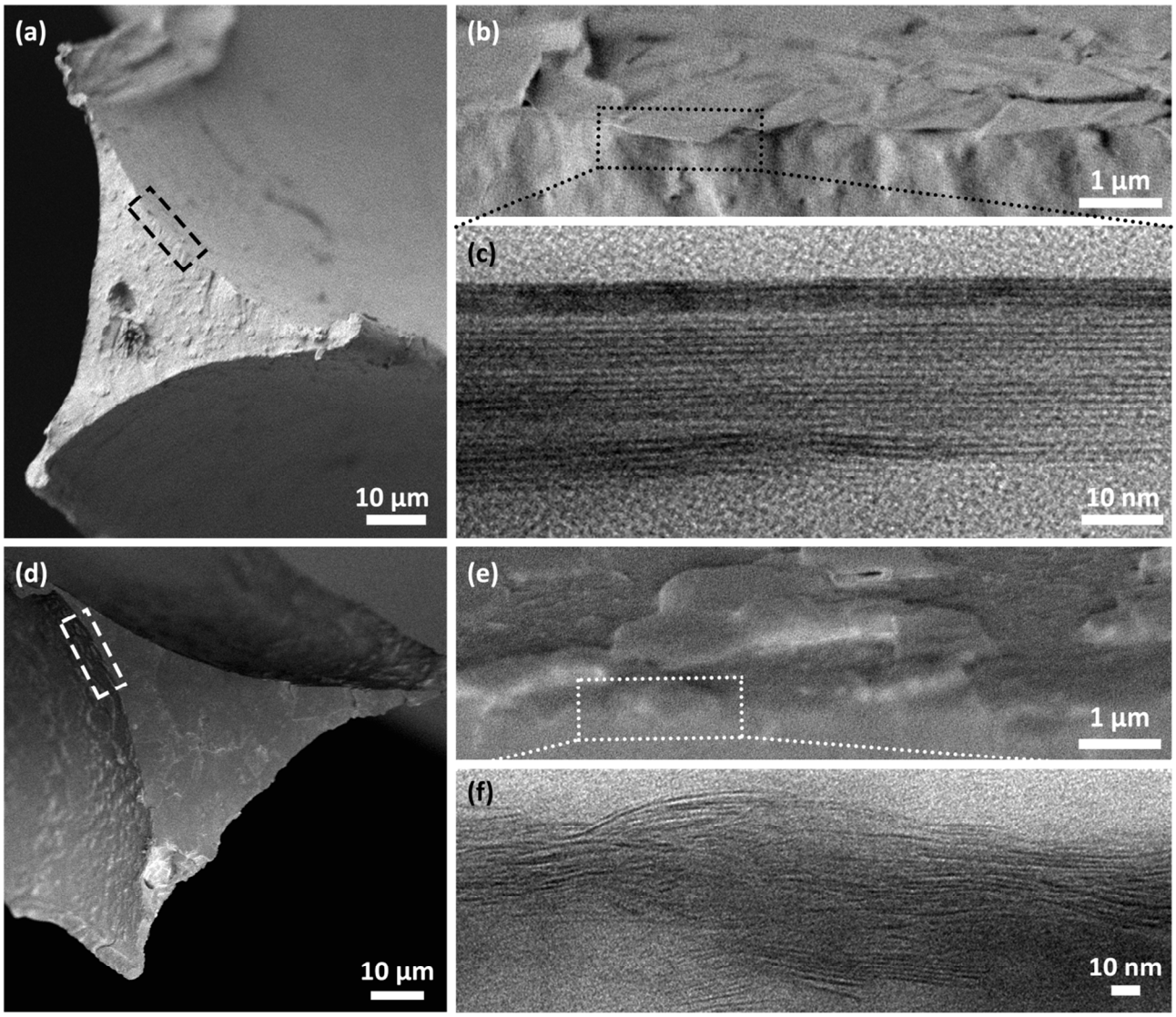

Fig. 3 SEM images of freeze-fractured polyurethane foam coated with 1 BL of a-b) PEI/VMT and d-e) PEI/MMT. TEM micrographs of polyurethane foam coated with 1 BL of c) PEI/VMT and f) PEI/MMT.

Flame retardant behavior

Butane torch testing. Nanobrick walls (i.e., polymer/clay LBL thin films), composed of either MMT or VMT bricks, were deposited on open-celled, flexible foam to evaluate the influence of nanoplatelet composition and aspect ratio on thermal stability. Nanocoating weight gain was determined by dividing the difference in weight of the foam before and after the coating was applied by the original weight of the polyurethane. Foam flammability was qualitatively screened by applying a butane torch to one side of a (5 x 5 x 2.54 cm) foam sample that was suspended in the air on a metal grating. Immediately upon contact with the flame, polyurethane melts away and the cellular structure is completely lost, forming liquid tar that melt drips and ignites paper placed directly below the grating.

All nanocoatings eliminated melt dripping. The flame from the butane torch burrowed a hole in both clay systems at 1 and 2 BL, while the 4 BL MMT-based coating fully maintained the foam's cellular structure and shape (see Fig. S1 in Supplemental Information). As a function of layers deposited, VMT-based coatings protected the underlying polyurethane better than MMT, with 2 BL VMT providing enough thermal shielding that undamaged foam was preserved under a thick char layer. When fire behavior is qualitatively compared as a function of nanocoating weight addition, 4 BL MMT-coated

samples (~3.3 wt.%) left more pristine foam remaining after torch testing than 1 BL VMT-coated samples (~3.2 wt.%). Pyrolysis molecules and heat have more gaps to breach and permeate through single BL MMT-based nanobrick walls because the bricks are an order of magnitude smaller. The additional polymer/clay layers necessary to normalize weight gain adds multiple MMT platelets with each additional BL. It is possible these additional layers not only significantly increase the thermal stability of the MMT-based nanobrick walls but also increase the tortuous path for combustion products to escape and feed the flame.

Cone calorimetry and thermal analysis. In an effort to quantitatively evaluate the thermal barrier properties of these polymer/clay thin films, control and coated (1, 2, and 4 MMT-BL; 1 and 2 VMT-BL) polyurethane foam was tested with standard cone calorimetry (ASTM E-1354-07). All samples were exposed to an external heat flux of 35 KW m^{-2}. While samples were subjected to this controlled radiant heat, heat and smoke release rates, production of toxic gas species, and mass loss data were collected as a function of time with an oxygen sensor, a laser photometer beam, CO_2/CO detection system, and a load cell. Fig. 4 shows heat release rate (HRR) and flammability data for six sample sets plotted as a function of the number of layers deposited (Fig. 4a) and as a function of coating weight addition (Fig. 4b). Control specimens ignited rapidly, and underwent polyurethane's characteristic two-step combustion process (i.e., thermosetting polymer boils, liquefies, and the cellular structure collapses, releasing large amounts of heat), which produces two distinct peak heat release rates (pkHRRs). The first peak is associated with the combustion of the isocyanate and the second higher peak is associated with the combustion of the polyol components.[47] As expected, immediately following high pkHRR, the remaining combustible material volatilizes and very little residue remains.

The most significant predictor of a fire hazard is heat release rate.[48] For both clay coating systems, increasing the number of bilayers deposited resulted in greater reductions in peak heat release rate and maximum average rate of heat emission (MARHE). pkHRR reports the highest rate of heat release, as determined via oxygen consumption calorimetry, and indicates the propensity of the flame

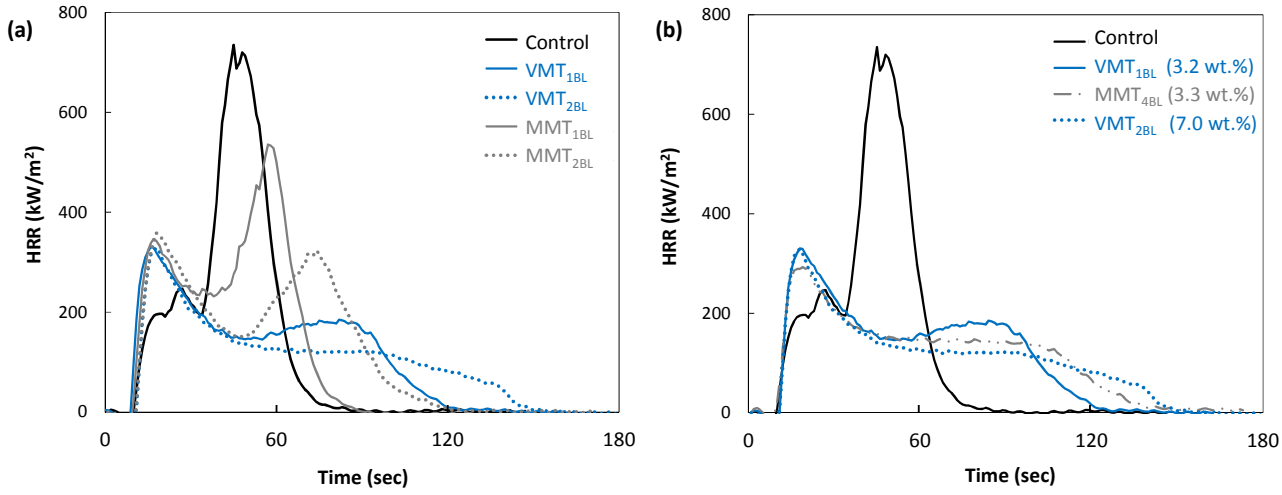

Fig. 4 Heat release rate as a function of time for control foam and foam coated with nanobrick wall thin films with varying a) number of layers deposited and b) coating weight addition.

Table 1. Cone calorimeter results for polyurethane foam samples.

Sample [units]	Wt. Gain [%]	pkHRR[a] [kW m^{-2}]	THR[b] [MJ m^{-2}]	Wt. Lost [%]	TSR[c] [m^2 m^{-2}]	MARHE[d] [kW m^{-2}]
Control		735 ± 11	19.5 ± 0.2	100	146 ± 4	318 ± 5
$(PEI/MMT)_1$	1.1 ± 0.2	531 ± 33	18.7 ± 0.6	94 ± 1	157 ± 14	273 ± 16
$(CH/MMT)_2$	1.5 ± 0.1	343 ± 15	19.2 ± 0.8	96 ± 1	130 ± 3	207 ± 6
$(CH/MMT)_4$	3.3 ± 0.3	298 ± 6	17.2 ± 0.5	92 ± 1	72 ± 7	170 ± 6
$(PEI/VMT)_1$	3.2 ± 0.2	339 ± 12	17.9 ± 0.6	87 ± 7	101 ± 12	195 ± 11
$(CH/VMT)_2$	7.0 ± 0.4	322 ± 7	17.1 ± 0.5	89 ± 1	61 ± 1	178 ± 4

[a]pkHRR = peak heat release rate; [b]THR = total heat release; [c]TSR = total smoke release; [d]MARHE = maximum average rate of heat emission

to self-propagate and/or spread to other materials in the absence of an external heating source. MARHE is a fire engineering parameter, defined as the total heat release normalized by time, which can be used to rank materials in terms of their ability to spread fire to other objects. In all cases, char yield and total heat release (THR) appear to be inversely related (Table 1). Higher char yield signifies that more of the sample is converted into less flammable solid residue, which diminishes the amount of specimen available as fuel. For both clay systems, increasing the number of bilayers deposited yielded greater reductions in total smoke release, which is noteworthy because deaths related to fire incidents commonly result from inhalation of toxic combustion products.[49]

After exposure to the cone heater, both 1 and 2 BL MMT-based systems rapidly smoked and ignited, but no liquefaction occurred. Surface char that formed from 1 BL MMT samples shrank during burning, leaving a final stiff char approximately 0.25 inches thick. Although 2 BL MMT nanocoated samples did not shrink during burning as much as single bilayer MMT, the second pkHRR curve shape suggests char formed was not sufficient to prevent underlying fuel from being converted into heat. 1 and 2 BL VMT and 4 BL MMT samples also smoked and ignited quickly after exposure to the cone heater, but these nanocoatings rapidly formed a thermally thick residue that prevented collapse and flow during burning. For these three systems, the first peak has the highest heat release rate, which is why the time from ignition to the pkHRR decreases from 40 s (uncoated, control PU) down to 13 s (coated PU). Although it is meaningful to understand how fast the sample reaches its maximum energy release after ignition, all three of these coating systems effectively decrease the flammability of the open-celled foam by decreasing the pkHRR and average HRR by at least 54%. 1 BL VMT sufficiently reduced the second pkHRR, but the other two systems (2 BL VMT and 4 BL MMT recipes) completely eliminated the peak and greatly extended the time the total heat was released. One bilayer MMT-based systems exhibited the highest overall flammability, whereas 4 BL MMT had the lowest overall pkHRR value (298 kW m^{-2}) and MARHE rating (170 kW m^{-2}) of the systems studied.

In a direct comparison of 1 BL polymer/clay thin films, VMT-based coatings reduce the pkHRR of polyurethane 36% more than MMT-based coatings (with respect to uncoated polyurethane). Although there is only a 6% reduction in pkHRR when comparing 2 BL VMT-based coatings to 2 BL MMT-based films, VMT bilayers suppress the second pkHRR and significantly extend the time it takes for total heat to be released. MMT bilayers simply alter the polyurethane decomposition cycle. In addition to having less thermally shielding material present in these 1 BL thin films, the average aspect ratio of montmorillonite platelets is an order of magnitude smaller than vermiculite, which generates more gaps for heat to permeate through and pyrolysis products to propagate out of the thin film. Increasing platelet aspect ratio in these thin film assemblies is known to impart improved gas barrier.[50-52] When nanocoating weight addition was normalized between the two clay systems, both 1 BL VMT and 4 BL MMT-based coatings had similar HRR curves, whose shape represents the typical thermally thick charring sample, but the montmorillonite system has the lowest pkHRR, THR, and TSR. Of all polymer/clay systems evaluated with cone calorimetry, the 2 BL VMT-based nanocoating has the greatest reduction in smoke release (58% relative to uncoated polyurethane samples), which further confirms the hypothesis that the barrier created with the high aspect ratio VMT platelets has fewer interfaces for pyrolysis volatiles and smoke to escape. Note that 1 BL MMT-based nanocoatings *increase* smoke release by 8% and 2 BL MMT-based nanocoatings only reduce smoke release by 11%.

Polymer nanocomposites typically fight fire through the condensed phase mechanism, interfering with a polymer's combustion cycle by forming a thermal shield of ceramic armor that prevents melt dripping when a heating source is applied.[53] As more MMT layers are deposited, the protective nature of the nanobrick wall coating increases, suggesting the effect of aspect ratio of clay diminishes. Thermogravimetric analysis reveals this thermally shielding residue at 400 °C, 500 °C, and 600 °C is equivalent for both a 1 BL VMT coating and 4 BL MMT (see Fig. S2 in Supplemental Information). It should be noted that the percent residue at each of the specified temperatures is greater than the amount of coating deposited on the polyurethane, signifying some of the foam has been converted to carbonized residue.

Both montmorillonite and vermiculite are 2:1 phyllosilicate minerals (i.e., their crystal structures have 1 octahedral hydroxide sheet between 2 tetrahedral silicate sheets) and have high cationic exchange capacity.[54,55] Despite their similarity, there are key differences between these clays that explain why MMT-based coatings require 4 bilayers to match the fire performance of a single polymer/vermiculite bilayer. VMT has an order of magnitude larger aspect ratio than MMT which reduces the number of interfaces pyrolysis products can escape through and/or heat can be transferred past. Partial clay exfoliation in solution, which results in platelet stacks depositing in the nanocoating, is another parameter that enhances fire retarding performance, as VMT itself intumesces.[56] Upon the addition of heat, bound water molecules (and possibly other combustion gases) expand and thermally exfoliate the vermiculite in the direction perpendicular to the platelet's longest dimension.[57] It has been suggested that iron present within vermiculite's tetrahedral layers also enhances the clay's thermal stability by acting as a radical trap and/or char catalyst site.[58-61]

Fig. S3 in Supplemental Information shows top-down and cross-sectional SEM micrographs of both 1 BL nanobrick wall systems and 4 BL MMT-coated samples after cone calorimetry testing, along with corresponding energy-dispersive X-ray spectroscopy (EDX). The residue of VMT-coated samples contained iron (in addition to expected carbon, nitrogen, oxygen, magnesium, aluminium, and silicon elemental peaks found in both clay sample sets) suggesting this element did participate in the condensed phase mechanism. If the metal ions did promote char formation (i.e., Lewis acid mechanism),[65] reduction of smoke release could also be attributed, in part, to the iron. The VMT slurry provided for this study contained silicon additives (this binder is reported to reduce smoke release at high temperatures).* In order to facilitate mixing between the silicon additives and the vermiculite, 0.1 wt.% phosphorous oligomer was added to the slurry. It is well known that phosphorous compounds (depending on their chemical structure and their interaction with polymer and/or added synergists) can

interfere in the combustion cycle in both the vapor and condensed phases. This interference occurs by volatilization into the gas phase (HPO_2•, PO•, PO_2•, and HPO•),[62] and scavenging H• and OH• radicals, or decomposing in the condensed phase by catalyzing char accumulation on the polymer surface.[53,63,64] No phosphorous peak was detected in the single bilayer VMT-coated samples before (and after) cone testing, suggesting the oligomer did get included in the layer-by-layer thin film and did not contribute to the fire performance. Fig. S4 and Table S1 in Supplemental Information show heat release rate curves (and corresponding fire performance data) for control foam and foam coated with 1 and 2 BL nanobrick wall thin films comprised of two types of vermiculite (vermiculite HTS-SE and vermiculite 963++). Vermiculite 963++ slurry does not contain chemical additives. All four HRR curves are representative of thermally thick charring materials, which display an initial high HR and then the HRR plateaus before terminating. Both 2BL VMT-based systems have lower overall flammability and smoke release than 1 BL VMT-based systems. Final chars of VMT-coated polyurethane retain their original shape and are black and fluffy. Nanobrick wall thin films with VMT-963++ as bricks have a slightly higher initial peak heat release rate for both 1 and 2 BL systems, but there is negligible change in THR. Although the silicone binder is reported to reduce smoke release at higher temperatures, it is more reasonable to assume that the performance difference in TSR for VMT-HTS-SE and VMT-963++ is related to nanocoating weight addition.

Experimental

Materials

Poly(acrylic acid) (PAA, M = 100 kg mol^{-1}, 35 wt.% in water) and branched polyethylenimine (PEI, M = 25 kg mol^{-1}) were purchased from Sigma-Aldrich (Milwaukee, WI), while chitosan (CH, M = 60 kg mol^{-1}, deacelylation 95%) was purchased from G.T.C. Union Group Ltd. (Qingdao, China). Sodium montmorillonite clay (MMT, trade name Cloisite Na+) was provided by Southern Clay Products, Inc. (Gonzales, TX) and formulated vermiculite HTS-SE (VMT, 15-16 wt.% in water) was supplied from Specialty Vermiculite (Cambridge, MA).* This type of VMT has 60% of particles ≤ 20 μm (≤ 25% particles are larger than 45 μm). Aqueous solutions of 1 wt.% PAA, 0.1 wt.% PEI, 0.1 wt.% CH, 1.0 wt.% MMT, and 1.0 wt.% VMT were prepared using deionized (DI) water and rolled for 12 h. Prior to deposition, the pH of each PAA and PEI solution was altered to 2 (using 2 M nitric acid) and 10 (using 1 M hydrochloric acid), respectively. CH was solubilized in acidic deionized water (pH 1.5), and then the pH of the cationic solution was raised to 6 prior to deposition (using 1 M sodium hydroxide). Both MMT and VMT clay suspensions were used at their unaltered pH (9.7 and 7.8, respectively). The PAA deposition functions as a surface treatment for polyurethane foam. The first bilayer for both nanobrick wall systems is PEI/clay, where the PEI deposition serves as a primer layer. All subsequent bilayers deposited on substrates are comprised of CH/clay.

Substrates

P-doped, single side polished (1 0 0) silicon wafers (University Wafer, South Boston, MA), with a thickness of 500 mm, were used as substrates for ellipsometric thickness measurements. Layers were incrementally deposited on 5 MHz Au/Ti-electrode quartz crystals (Maxtek, Inc., Cypress, CA) to obtain mass deposited per layer using a quartz crystal microbalance. Polyether-based polyurethane foam (type 1850), with a density of 1.75 lbs ft^{-1}, was purchased from Future Foam (High Point, NC).

Layer-by-layer deposition

Fabrication of the multilayer flame retardant nanocoatings on two-dimensional substrates (silicon wafers or Au/Ti crystals) for thin film characterization was carried out using a home-built dipping system, where flat, 2D substrates were immersed in solutions for reported times and rinsed with deionized water and dried with filtered air.[66] Fabrication of the multilayer thin films for 3D substrates was carried out by fully compressing foam in solutions three times with a thin sheet of acrylic in an effort to achieve a more uniform compression across the surface. Excess solution (or rinse water) was removed from the foam with hand crank wringers. This coating technique significantly improved the consistency in weight addition of the nanocoating (relative to squeezing foam by hand). Polyurethane was first submerged in PAA solution for 30 s to enhance the adhesion between the foam surface and the nanocoating. In pH 2 poly(acrylic acid) solution, carboxylic acid groups on PAA hydrogen bond with the polyurethane surface. Treated substrates were then dipped in the PEI solution for 5 min, rinsed in DI water, and wrung out. When the PAA-coated surface was exposed to pH 10 solution, the charge density of the weak polyelectrolyte increased and caused PAA chains to attract PEI to the surface via hydrogen bonding (and possibly electrostatic attraction). This deposition procedure was followed by an identical dipping, rinsing, and wringing dry for the clay suspension. If subsequent polymer/clay layers were deposited, the same coating procedure was followed with 1-min CH/clay dip times, until the desired number of layers was deposited, as shown in Fig. 5. Foam samples were dried in an oven at 70 °C for 3 h immediately following deposition.

Thin film characterization

An alpha-SE Ellipsometer (J.A. Woollman Co., Inc., Lincoln, NE), with a 632.8 nm laser, was used to measure film thicknesses on polished silicon wafers. A Maxtek Research Quartz Crystal Microbalance (QCM, Cypress, CA) was used to monitor mass deposition of individual layers deposited on Au/Ti crystals in order to calculate total film density. Small slices taken from single bilayer coated foam (PEI/MMT and PEI/VMT) were embedded in Epofix (EMS, Hatfield, PA) and left to cure overnight at room temperature. Thin (< 90 nm) gold sections were trimmed using a microtome and

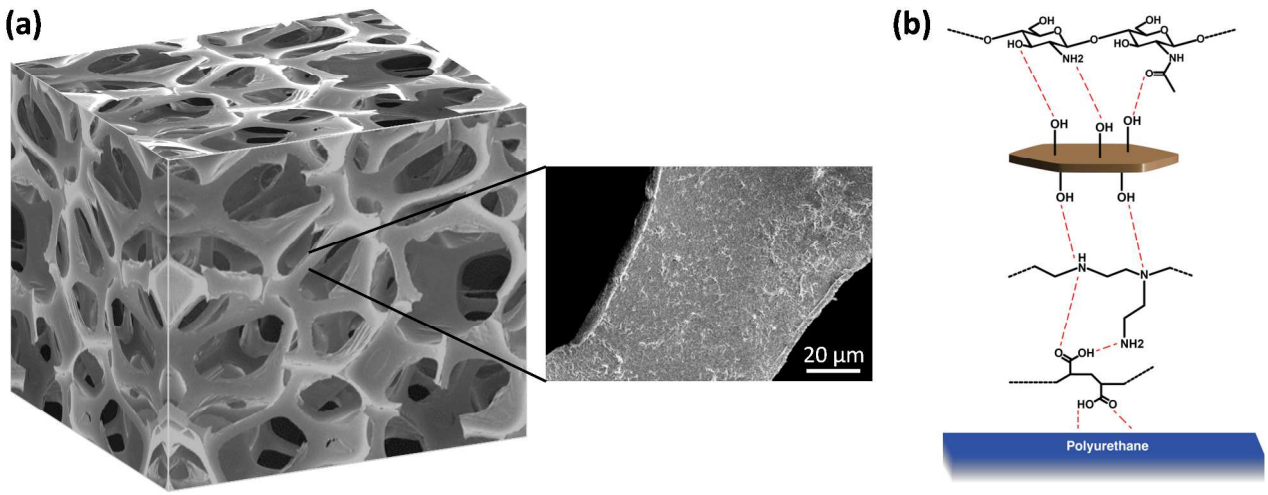

Fig. 5 Schematic of the coated foam (inset: SEM image of 4 BL MMT-based nanobrick wall on polyurethane). b) Chemical structures of the nanobrick wall components after deposition (PAA surface treatment, PEI primer, clay, and chitosan).

were picked up on lacey Formvar-coated 300 mesh copper grids. Thin film cross-sections were imaged with a Tecnai G2 F-20 TEM (FEI, Hillsboro, OR) at an operating voltage of 200 kV and calibrated magnifications. Coated thin films, deposited on PU substrates, were mounted on aluminum imaging stubs and thinly sputter coated with 5 nm of platinum/palladium (Pt/Pd) alloy in preparation for surface images that were acquired with a field-emission scanning electron microscope (FESEM) (Model JSM-7500F, JEOL; Tokyo, Japan). Energy-dispersive X-ray spectroscopy (EDX) samples were not sputter coated with Pt/Pd. The elemental spectra in Fig. S3 (in Supporting Information) were acquired with the FESEM.

Thermal stability, flammability, and combustibility of foam

Fire behavior of the nanocoating was qualitatively screened with the direct flame of a butane micro hand torch (MT-76K, Master Appliance Corp., Racine, WI) for 10 s (the approximate blue flame temperature is 2500 °F). A Q50 Thermogravimetric Analyzer (TGA; TA Instruments, New Castle, DE) was used to measure the thermal stability of control and coated polyurethane foam. Each ~ 30 mg sample was tested in an air atmosphere from room temperature up to 640 °C, with a heating rate of 10 °C min^{-1}. Cone calorimetry was operated according to standardized procedures (ASTM E-1354-11) at the University of Dayton Research Institute using a FTT Dual Cone Calorimeter (exhaust flow of 24 L s^{-1}). Samples (10 x 10 x 2.5 cm) were placed in a pan constructed from aluminium foil and exposed to a heat flux of 35 kW m^{-2}, with an uncertainty of 5% in HRR and 2 s in time.

Conclusions

Flame retardant thin films deposited on open-celled, flexible polyurethane foam, using layer-by-layer assembly of polymeric mortar and vermiculite clay platelets, were shown to dramatically improve fire performance through the condensed phase mechanism. A single bilayer of PEI and formulated-vermiculite clay, which adds only 3.2 wt.% to the foam, successfully prevented formation of a melt pool of burning polymer and reduced peak heat release rate and total smoke release by 54% and 31%, respectively. Four polymer/MMT bilayers are needed to surpass the fire protection properties of VMT's single bilayer barrier. These exceptional fire protection properties of VMT-coated foam are largely attributed to the self-intumescing and heat-shielding characteristics of this high aspect ratio clay. The effect of the added phosphorous on flammability performance is negligible. This first ever report of vermiculite in a LbL-constructed nanobrick wall for fire protection provides an exciting opportunity for imparting environmentally-benign anti-flammability to complex polymer substrates. In some instances, just one or two bilayers may be all that is necessary to impart adequate protection, making this system relatively fast and simple.

Acknowledgements

The authors acknowledge the Fire Research Division (FRD) of the Engineering Laboratory (EL) at the National Institute of Standards and Technology (NIST) for financial support of this work, the Microscopy & Imaging Center (MIC) for TEM imaging assistance, and the Materials Characterization Facility (MCF) at Texas A&M for SEM/EDX imaging assistance.

Notes and references

[a] Department of Mechanical Engineering; Department of Materials Science & Engineering; and Department of Chemistry, Texas A&M

University, 3123 TAMU, College Station, Texas 77843, USA. E-mail: (jgrunlan@tamu.edu)
[b] Department of Chemical Engineering, Ben-Gurion University of the Negev, 84105 Berr-Sheva, Israel.

† Electronic Supplementary Information (ESI) available: [Supplementary Information contains images of foam coated with both nanobrick wall thin films before and after torch testing, TGA data for control foam and foam coated with both nanobrick wall thin film recipes, SEM micrographs of both 1 BL nanobrick wall systems and 4 BL MMT-coated samples after cone calorimetry testing and corresponding elemental spectra, cone calorimetry data of nanobrick wall thin films composed of formulated vermiculite bricks (HTS-SE) and vermiculite bricks without additives (963++).]. See DOI: 10.1039/b000000x/

* Specialty Vermiculite does not disclose the exact chemistry of Vermiculite-HTS-SE. It should be noted that the additive concentration is very low. Supplementary Information displays heat release rate curves that compare polyurethane coated with 1 and 2 BL vermiculite nanobrick wall thin films (1 set comprised of VMT-HTS-SE, used in the manuscript, and the second set comprised of VMT 963++, which does not contain chemical additives). Cone calorimetry data shows nanobrick wall thin films comprised of formulated vermiculite have the same flame retardant behavior as the thin films created from the vermiculite slurry without the additives. This suggests the additives do not influence the observed flame retardant performance.

1 G. Decher, in *Multilayer Thin Films: Sequential Assembly of Nanocomposite Materials*, Vol. 1 (Eds: G. Decher, J. Schlenoff), Wiley-VCH, Weinheim **2012**.
2 K. Ariga, Y. Yamauchi, G. Rydzek, Q. M. Ji, Y. Yonamine, K. C. W. Wu, J. P. Hill, *Chem. Lett.* **2014**, *43*, 36.
3 P. Bertrand, A. Jonas, A. Laschewsky, R. Legras, *Macromol. Rapid Commun.* **2000**, *21*, 319.
4 P. Podsiadlo, B. S. Shim, N. A. Kotov, *Coord. Chem. Rev.* **2009**, *253*, 2835.
5 M. A. Priolo, D. Gamboa, J. C. Grunlan, *ACS Appl. Mater. Interfaces* **2009**, *2*, 312.
6 M. Priolo, K. Holder, S. Greenlee, B. Stevens, J. Grunlan, *Chem. Mater.* **2013**, *25*, 1649.
7 M. A. Priolo, K. M. Holder, D. Gamboa, J. C. Grunlan, *Langmuir* **2011**, *27*, 12106.
8 A. J. Svagan, A. Åkesson, M. Cárdenas, S. Bulut, J. C. Knudsen, J. Risbo, D. Plackett, *Biomacromolecules* **2012**, *13*, 397.
9 G. Findenig, S. Leimgruber, R. Kargl, S. Spirk, K. Stana-Kleinschek, V. Ribitsch, *ACS Appl. Mater. Interfaces* **2012**, *4*, 3199.
10 J. H. Choi, Y. W. Park, T. H. Park, E. H. Song, H. J. Lee, H. Kim, S. J. Shin, V. Lau Chun Fai, B.-K. Ju, *Langmuir* **2012**, *28*, 6826.
11 M. A. Priolo, D. Gamboa, K. M. Holder, J. C. Grunlan, *Nano Lett.* **2010**, *10*, 4970.
12 E. L. Cussler, S. E. Hughes, W. J. Ward, R. Arias, *J. Membr. Sci.* **1988**, *38*, 161.
13 P. Tzeng, C. R. Maupin, J. C. Grunlan, *J. Membr. Sci.* **2014**, *452*, 46.
14 D. A. Hagen, C. Box, S. Greenlee, F. Xiang, O. Regev, J. C. Grunlan, *RSC Adv.* **2014**, *4*, 18354.
15 R. Ou, J. Zhang, Y. Deng, A. Ragauskas, *J. Appl. Polym. Sci.* **2007**, *105*, 1987.
16 L. J. Bonderer, A. R. Studart, J. Woltersdorf, E. Pippel, L. J. Gauckler, *J. Mater. Res.* **2009**, *24*, 2741.
17 P. Podsiadlo, A. K. Kaushik, E. M. Arruda, A. M. Waas, B. S. Shim, J. Xu, H. Nandivada, B. G. Pumplin, J. Lahann, A. Ramamoorthy, N. A. Kotov, *Science* **2007**, *318*, 80.
18 P. Podsiadlo, M. Michel, J. Lee, E. Verploegen, N. Wong Shi Kam, P. T. Hammond, V. Ball, Y. Qi, A. J. Hart, N. Kotov, *Nano Lett.* **2008**, *8*, 1762.
19 S. b. Peralta, J.-L. Habib Jiwan, A. Jonas, *ChemPhysChem* **2009**, *10*, 137.
20 V. Ball, K. Apaydin, A. Laachachi, V. Toniazzo, D. Ruch, *Biointerphases* **2012**, *7*.
21 J. Lutkenhaus, E. Olivetti, E. Verploegen, B. Cord, D. Sadoway, P. Hammond, *Langmuir* **2007**, *23*, 8515.
22 F. Hua, T. Cui, Y. M. Lvov, *Nano Lett.* **2004**, *4*, 823.
23 M. de Villiers, D. Otto, S. Strydom, Y. Lvov, *Adv. Drug Delivery Rev.* **2011**, *63*, 701.
24 J. Min, R. Braatz, P. Hammond, *Biomaterials* **2014**, *35*, 2507.
25 A. Zhuk, R. Mirza, S. Sukhishvili, *ACS Nano* **2011**, *5*, 8790.
26 Y.-C. Li, J. Schulz, S. Mannen, C. Delhom, B. Condon, S. Chang, M. Zammarano, J. C. Grunlan, *ACS Nano* **2010**, *4*, 3325.
27 A. Laachachi, V. Ball, K. Apaydin, V. Toniazzo, D. Ruch, *Langmuir* **2011**, *27*, 13879.
28 S. Chang, R. P. Slopek, B. Condon, J. C. Grunlan, *Ind. Eng. Chem. Res.* **2014**, *53*, 3805.
29 K. Apaydin, A. Laachachi, V. Ball, M. Jimenez, S. Bourbigot, V. Toniazzo, D. Ruch, *Polym. Degrad. Stab.* **2013**, *98*, 627.
30 S. V. Levchik, E. D. Weil, *Polymer International* **2004**, *53*, 1585.
31 M. Zanetti, T. Kashiwagi, L. Falqui, G. Camino, *Chem. Mater.* **2002**, *14*, 881.
32 A. A. Cain, C. R. Nolen, Y.-C. Li, R. Davis, J. C. Grunlan, *Polym. Degrad. Stab.* **2013**, *98*, 2645.
33 G. Laufer, C. Kirkland, A. A. Cain, J. C. Grunlan, *ACS Appl. Mater. Interfaces* **2012**, *4*, 1643.
34 Y. S. Kim, R. Harris, R. Davis, *ACS Macro Lett.* **2012**, *1*, 820.
35 Y. S. Kim, Y.-C. Li, W. M. Pitts, M. Werrel, R. D. Davis, *ACS Appl. Mater. Interfaces* **2014**, *6*, 2146.
36 H. Singh, A. K. Jain, *J. Appl. Polym. Sci.* **2009**, *111*, 1115.
37 Y. Li, J. Kim, R. Shields, Davis, *J. Mater. Chem. A* **2013**, *1*, 12987.
38 Y. T. Park, Y. Qian, C. I. Lindsay, C. Nijs, R. E. Camargo, A. Stein, C. W. Macosko, *ACS Appl. Mater. Interfaces* **2013**, *5*, 3054.
39 C. Aulin, G. Salazar Alvarez, T. Lindstrom, *Nanoscale* **2012**, *4*, 6622.
40 V. Mittal, *J. Compos. Mater.* **2008**, *42*, 2829.
41 S. Takahashi, M. Farrell, H. A. Goldberg, C. A. Feeney, D. P. Karim, K. O'Leary, D. R. Paul, *Polymer* **2006**, *47*, 3083.
42 T. Guin, M. Guin, D. Krecker, J. Hagen, Grunlan, *Langmuir* **2014**, *30*, 7057.
43 M. A. Priolo, K. M. Holder, S. M. Greenlee, J. C. Grunlan, *ACS Appl. Mater. Interfaces* **2012**, *4*, 5529.
44 H. J. Ploehn, C. Y. Liu, *Ind. Eng. Chem. Res.* **2006**, *45*, 7025.
45 S. S. Shiratori, M. F. Rubner, *Macromolecules* **2000**, *33*, 4213.
46 Y. H. Yang, M. Haile, Y. T. Park, F. A. Malek, J. C. Grunlan, *Macromolecules* **2011**, *44*, 1450.
47 R. H. Krämer, M. Zammarano, G. T. Linteris, U. W. Gedde, J. W. Gilman, *Polym. Degrad. Stab.* **2010**, *95*, 1115.
48 V. Babrauskas, R. D. Peacock, *Fire Saf. J.* **1992**, *18*, 255.
49 M. Stefanidou, S. Athanaselis, C. Spiliopoulou, *Inhalation Toxicol.* **2008**, *20*, 761.
50 Y.-H. Yang, L. Bolling, M. A. Priolo, J. C. Grunlan, *Adv. Mater.* **2013**, *25*, 503.
51 M. Priolo, K. Holder, S. Greenlee, J. Grunlan, *ACS Appl. Mater. Interfaces* **2012**, *4*, 5529.
52 F. Xiang, P. Tzeng, J. S. Sawyer, O. Regev, J. C. Grunlan, *ACS Appl. Mater. Interfaces* **2013**, *6*, 6040.
53 F. Laoutid, L. Bonnaud, M. Alexandre, J.-M. Lopez-Cuesta, P. Dubois, *Mater. Sci. Eng.,R* **2009**, *63*, 100.
54 O. Abollino, A. Giacomino, M. Malandrino, E. Mentasti, *Appl. Clay Sci.* **2008**, *38*, 227.
55 F. Annabi-Bergaya, *Microporous Mesoporous Mater.* **2008**, *107*, 141.
56 Q. A. Ren, Y. Zhang, J. A. Li, J. C. Li, *J. Appl. Polym. Sci.* **2011**, *120*, 1225.
57 C. Marcos, I. Rodríguez, *Appl. Clay Sci.* **2014**, *90*, 96.
58 X. T. Chen, Y. L. Yin, J. Lu, X. H. Chen, *J. Fire Sci.* **2014**, *32*, 179.
59 M. Du, B. Guo, D. Jia, *Eur. Polym. J.* **2006**, *42*, 1362.
60 T. Kashiwagi, E. Grulke, J. Hilding, K. Groth, R. Harris, K. Butler, J. Shields, S. Kharchenko, J. Douglas, *Polymer* **2004**, *45*, 4227.
61 J. Zhu, F. M. Uhl, A. B. Morgan, C. A. Wilkie, *Chem. Mater.* **2001**, *13*, 4649.
62 V. Babushok, W. Tsang, *Combust. Flame* **2000**, *123*, 488.
63 E. D. Weil, in *Flame-Retardant Polymeric Materials*, Vol. 2 (Eds: M. Lewin, S. M. Atlas, E. M. Pearce), Plenum Press, New York **1978**, 103.
64 A. B. Morgan, J. W. Gilman, *Fire Mater.* **2013**, *37*, 259.

65 U. Braun, B. Schartel, M. A. Fichera, C. Jäger, *Polym. Degrad. Stab.* **2007**, *92*, 1528.
66 W.-S. Jang, J. C. Grunlan, *Rev. Sci. Instrum.* **2005**, *76*.

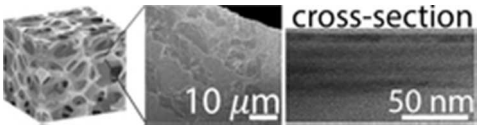

Single bilayer polymer/clay nanobrick wall self-assembled thin films, deposited as a continuous coating on open-celled polyurethane foam, cut peak heat release rate in half with only 3.2 wt% addition.
19x4mm (300 x 300 DPI)